Available online at www.sciencedirect.com

ScienceDirect

journal homepage: http://www.elsevier.com/locate/rpor

Original research article

Evaluation of reproducibility of tumor repositioning during multiple breathing cycles for liver stereotactic body radiotherapy treatment

Ludovic Bedos, Olivier Riou, Norbert Aillères, Antoine Braccini, Jessica Molinier, Carmen Llacer Moscardo, David Azria, Pascal Fenoglietto*

Radiation Oncology Department, Institut régional du Cancer de Montpellier (ICM), Val d'Aurelle, 208 avenue des Apothicaires, 34298 Montpellier cedex 5, France

ARTICLE INFO

Article history:
Received 5 November 2015
Received in revised form
15 June 2016
Accepted 23 July 2016
Available online 12 November 2016

Keywords:
Gated VMAT
Intrafraction target motion verification
Respiratory gating

ABSTRACT

Aim: To evaluate the tumor repositioning during gated volumetric modulated arc therapy (VMAT) for liver stereotactic body radiotherapy(SBRT) treatment using implanted fiducial markers and intrafraction kilovoltage (kV) images acquired during dose delivery.

Materials and methods: Since 2012, 47 liver cancer patients with implanted fiducial markers were treated using the gated VMAT technique with a Varian Truebeam STx linear accelerator. The fiducial markers were implanted inside or close to the tumor target before treatment simulation. They were defined at the maximum inhalation and exhalation phases on a 4-dimensionnal computed tomography (4DCT) acquisition. During the treatment, kV images were acquired just before the beam-on at each breathing cycle at maximum exhalation and inhalation phases to verify the fiducial markers positions. For the five first fractions of treatment in the first ten consecutive patients, a total of 2705 intrafraction kV images were retrospectively analyzed to assess the differences between expected and actual positions of the fiducial markers along the cranio-caudal (CC) direction during the exhalation phase.

Results: The mean absolute intrafractional fiducial marker deviation along the CC direction was 1.0 mm at the maximum exhalation phase. In 99%, 95% and 90% cases, the fiducial marker deviations were ≤4.5 mm, 2.8 mm and 2.2 mm, respectively.

Conclusion: Intrafraction kV images allowed us to ensure the consistency of tumor repositioning during treatment. In 99% cases, the fiducial marker deviations were ≤4.5 mm corresponding to our 5 mm treatment margin. This margin seems to be well-adapted to the gated VMAT SBRT treatment in liver disease.

* *Corresponding author.*
E-mail address: ludovic.bedos@icm.unicancer.fr (L. Bedos).

http://dx.doi.org/10.1016/j.rpor.2016.07.007
1507-1367/

1. Background

Stereotactic Body Radiation Therapy (SBRT) is an effective treatment procedure allowing the delivery of high radiation doses in a few fractions leading to a high biological effective dose.[1] The delivered doses are strictly conformed to the target with a rapid fall-off away from the tumor, protecting the surrounding tissue, and the administration of high doses thus requires a very accurate dose delivery to the tumor. For abdominal tumors, the intrafraction motion provides some imprecision in the dose delivery. In liver SBRT, the main challenge is to take into account these motions. Liver motion is complex, consisting of translations, rotations and hysteresis. It is mostly related to breathing and is usually the largest in the cranio-caudal (CC) direction.[2] Kitamura et al. analyzed the liver tumor motion under tidal breathing and showed a tumor motion up to 4 mm (range 1–12 mm), 9 mm (range 2–19 mm) and 5 mm (range 2–12 mm) in the left–right (LR), CC and anterior–posterior (AP) directions, respectively.[2,3]

Several techniques can be used to manage tumor motion, such as active breath control, abdominal compression, respiratory gating and real-time tumor tracking.[4–9] In this study, we used the respiratory gating technique with an external surrogate placed on the patient's abdominal wall associated with implanted fiducial markers to manage liver motion.[5,10] The aim of this technique is to limit the radiation exposure during specific phases of the breathing cycle and to create a correlation model between the internal target motion and the external surrogate (skin surface), and finally to control the radiation beam delivery thanks to the external surrogate signal.

Previous studies have shown that the position of the tumor changes both between the treatment fractions (interfraction) and within a single treatment fraction (intrafraction).[11–15]

Park et al. analyzed the interfraction and intrafraction liver motion variability constructing a 3-dimensional motion trajectory of the fiducial markers implanted, at different sites in the liver and as a function of the breathing cycle. They reported, for 20 patients, a range of motion of 3.0 ± 2.0 mm, 5.1 ± 3.1 mm and 17.9 ± 5.1 mm using the planning 4-dimensionnal computed tomography (4DCT), and of 2.8 ± 1.6 mm, 5.3 ± 3.1 mm, and 16.5 ± 5.7 mm using the cone-beam computed tomography (CBCT), for the LR, AP and CC directions, respectively. The authors found that the breathing-induced AP and CC motions were highly correlated. They also reported a significant variation during the interfractional gating window, with the largest having 29.4–56.4% range between fractions.[12] Worm et al. described mean 3D intrafraction and intrafield motion ranges of internal markers during liver SBRT of 17.6 mm (range 5.6–39.5 mm) and 11.3 mm (range 2.1–35.5 mm), respectively, using standard X-ray imagers.[13]

In a recent study, Poulsen et al. used intrafraction kilovoltage (kV) imaging during volumetric-modulated arc therapy (VMAT) liver SBRT to estimate the intra-treatment target motion and to reconstruct the delivered target dose. They estimated that the intrafraction motion caused a mean 3D target position error of 2.9 mm and a mean D_{95} reduction of 6.0%.[14]

Interfraction uncertainties have been well reduced thanks to the daily use of image-guided setup techniques, such as kV imaging, fluoroscopy and kV CBCT. Intrafractional target motion verification is the new challenge to achieve. Indeed, it is crucial to make sure that the tumor always stays inside the planning target volume (PTV) when the radiation beam is turned on during the dose delivery. Because liver tumors cannot be visualized by kV images, intrafractional target motion verification relies on implanted fiducial markers. These can be used during the patient's setup and for the tumor motion verification as they are implanted inside or close to the target.[16] Recent report evaluated the geometric accuracy of the surrogate-based gated VMAT with a respiratory phantom and also on real patients cases including liver tumors.[17] Li et al. showed in a phantom study a high geometric accuracy (average error of 0.8 mm in the CC direction) when no target-surrogate relation changes occurred during the treatment. However, including a phase shift of 5% and 10% increased the average errors to 2.3 and 4.7 mm, respectively. The same authors obtained similar trend with real human respiratory curves. For the patient study, they obtained an average intrafraction positioning errors of 0.8, 0.9, and 1.4 mm in the LR, AP and CC directions, respectively.[17]

In our study, data sets of kV images acquired during the dose delivery using the Varian Novalis Truebeam Stx Linac and the Intrafraction Motion Review software (IMR) (Varian Medical Systems, Palo Alto, CA, USA) were used to evaluate the reproducibility of tumor repositioning during multiple breathing cycles during the liver SBRT treatment. The purpose of this evaluation was to determine if the internal target volume (ITV)/PTV safety margin used in our institution was appropriate and if it could be reduced.

Table 1 – Patients characteristics.

Patient index	Sex	Age (y)	PTV dose (Gy)	V_{PTV} (cm^3)
1	F	85	5 × 10	106.3
2	F	59	5 × 10	66.7
3	M	62	5 × 10	55.7
4	F	82	8 × 5	224.3
5	M	70	10 × 5	141.2
6	M	56	10 × 5	367.2
7	M	63	10 × 5	83.5
8	F	64	5 × 10	18.9
9	F	81	5 × 10	93.4
10	M	65	5 × 10	39.1

2. Materials and methods

2.1. *Patients, treatment simulation and planning*

Since 2012, 47 liver cancer patients with implanted fiducial markers were treated using the gated VMAT SBRT technique delivered using a Novalis Truebeam STx Linac. The present study was based on intrafraction kV images data from the first 10 patients treated with this technique (Table 1).

The fiducial markers were implanted inside or close to the tumor target before the treatment simulation. Most of the patients had two to three fiducial markers implanted (Visicoil, IBA) and some of them presented with multiple surgical clips or prostheses due to a previous surgery. The implantation procedure was made 1–2 weeks before the planning scan allowing

Fig. 1 – Marker points representing the maximum position of the fiducial markers in the inhale and exhale phases.

the fiducial positions to be stabilized. The fiducial markers were used for consistency verification of the liver motion and not necessarily for patient set-up. No minimum number of markers positioned in a specific geometry was required to allow treatment of the patients.

For the treatment simulation and delivery, the patients were placed in the supine position on a personalized body shape cushion (Moldcare, Circo) with the arms above the head. The patients breathed freely with no coaching before treatment simulation. For each patient, an injected 3DCT and a 4DCT scan were acquired using an Optima CT580 16-slice CT scanner (GE Medical Systems). The Real-time Position Management (RPM) system was used to record the respiratory signal and synchronize it to the scan acquisition. The 4DCT was acquired in the axial cine mode with a slice thickness of 2.5 mm. The 4DCT data were sorted into 10 phases of CT images with 0% and 50% representing the maximum inhalation and exhalation of the breathing cycle, respectively. An average intensity projection (Ave-IP), maximum intensity projection (MIP) and minimum intensity projection (Min-IP) scans were also generated.

Before the treatment planning, two to three more 4DCT scans were acquired over 10 days for each patient in order to study the reproducibility of the liver motion and of the fiducial markers motions between each other.

The gross tumor volume (GTV) was delineated on the injected 3DCT scan by a radiation oncologist. The ITV was defined on the Ave-IP CT scan using the study of the fiducial markers motions thanks to the dynamic CT scans (10 phases CT images), and the MRI acquisitions in deep inspiration and deep expiration breath hold, and 4DCT-PET. The ITV was determined to encompass the full range of respiratory motion. The PTV was created by adding a 5 mm isotropic margin from the ITV to account for setup inaccuracies and intrafraction tumor shifts. Organs at risks were delineated on the Ave-IP CT scan.

The fiducial markers were delineated on the maximum inhalation (0%) and exhalation (50%) phase CT scans representing their extreme positions, and on the MIP scan representing their integral motion. The Ave-IP CT scan was used as the planning CT.

Six Mega-Voltage (MV) VMAT (RapidArc) plans using the Eclipse treatment planning system (Varian Medical Systems, Palo Alto, CA, USA) were created, consisting of two half-arc fields used to avoid contralateral organs with a maximum dose rate of 600 monitor units/min. The dose calculations were carried out on the Ave-IP CT scan using the Anisotropic Analytical algorithm. The choice of the fractionation scheme was risk-adapted, dictated by the proximity to critical structures and mainly to the radiation-induced liver disease risk. The fractionation scheme was as follows: 5×10 Gy and 10×5 Gy delivered in two weeks. Plans were normalized such that a minimum of 95% of the PTV received 95% of the prescription dose, and such that the maximum dose (D2%) in the PTV was limited to 107% of the prescribed dose, *i.e.* a uniform PTV dose distribution.

For each fiducial marker, two marker points were placed to represent their extreme positions encompassing the global motion of the target defining the ITV (Fig. 1).

2.2. *Patient setup and verification*

Daily, for each patient, the RPM block was fixed to the patient's abdomen surface at the same place than the treatment simulation. The breathing signal generated by this block was recorded. An upper and lower gating threshold was defined surrounding this breathing signal, representing the daily breathing cycle amplitude.

The patient was first set up acquiring a CBCT scan according to a pelvis acquisition protocol (125 kV, 1056 mA s). The patient images were registered based on the liver information and on the fiducial marker positions. Because of the CBCT acquisition time (about 60 s), an average representation of the organs and tumor motions were included in those images. Consequently, the ITV of the day represented on the CBCT acquisition was compared to the planning ITV on the Ave-IP reference CT scan. This process leads to a correlation model between internal and external information. If the information were in good agreement, the daily breathing cycle amplitude was validated. The internal tumor and fiducial markers motions represented by the external RPM block were similar to those defined during the treatment planning.

During the second setup step, two orthogonal kV images were acquired, first at the maximum exhalation phase and then at the maximum inhalation phase (Fig. 2). The aim of those acquisitions was to verify the extreme positions of the ITV by checking the positions of the fiducial markers and

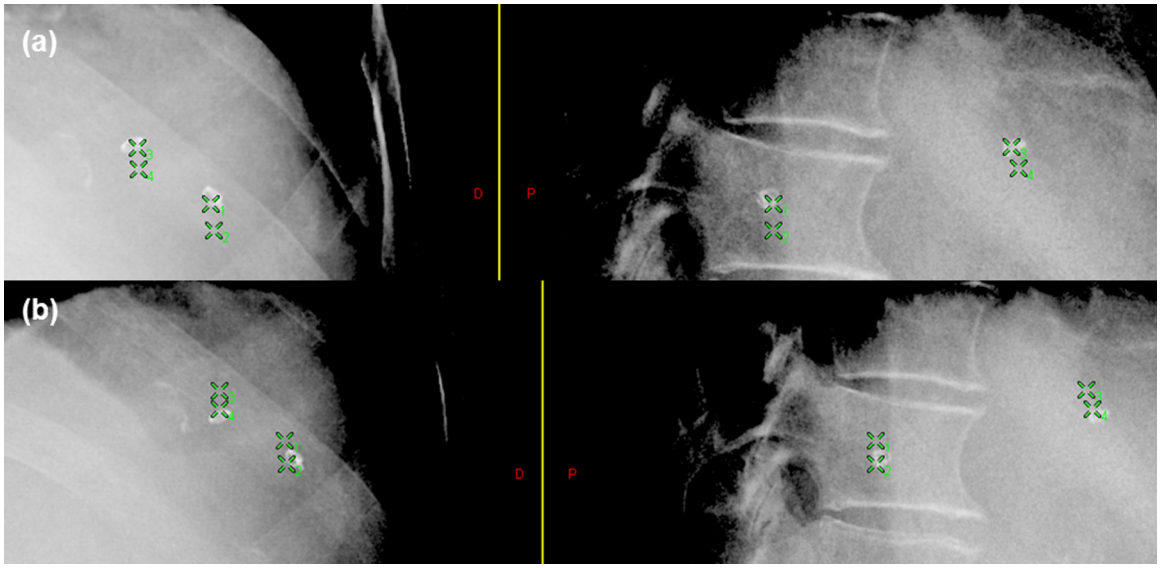

Fig. 2 – Two orthogonal kV images acquired at the maximum exhalation phase (a) and at the maximum inhalation phase (b). Upper and lower green cross represent the expected position in exhale phase and inhale phase, respectively. (For interpretation of the references to color in this figure legend, the reader is referred to the web version of this article.)

compare them with the expected positions according to the planning step.

The orthogonal kV images at the maximum exhalation phase were acquired first because it is the most reproducible phase and because it allows the adjustment of a baseline shift if necessary. If it was the case, and because of the spatial resolution accuracy is better than for the CBCT scan, refining the patient setup was allowed.

The orthogonal kV images at the maximum inhalation phase were then acquired, and the marker positions were compared again. At this stage, refining the patient setup was not authorized because of the eventuality of inhalation-amplitude changes. If the marker positions did not correspond to their expected positions, an adjustment of the gating threshold was performed, *i.e.* the total breathing amplitude was not used for the treatment (Figs. 3 and 4).

2.3. *Treatment delivery and intrafraction kV images*

The MV beam was triggered by the RPM system. The amplitude-based gating was used for all the treatments. During the gated VMAT delivery, the beam was turned on/off automatically when the breathing signal crossed the gating threshold, and a kV image (75 kV, 4 mA s, 0.3 mGy/image)[18] was acquired when the signal entered the gate just before MV beam on. That information allowed to continuously verify the consistency of the daily breathing cycle model controlling that the external–internal correlation still remained in good concordance.

The fiducial markers positions were compared to their expected positions in real time applying a 5 mm tolerance limit corresponding to the ITV/PTV margin. If the fiducial markers were shifted, the beam was turned off manually and kV images were still acquired until the markers came back to an acceptable position. Otherwise the MV beam was stopped and the patient was aligned again.

2.4. *Motion analysis*

The intrafraction kV images were used retrospectively to verify and evaluate the reproducibility of the tumor repositioning during gated VMAT treatment because they were acquired just before MV beam-on at each period of the breathing cycle. This analysis of the tumor motion was achieved by studying the marker position motions as they were implanted inside or close to the tumor target. The marker positions estimated from the kV images were compared to their reference positions defined on the orthogonal kV images during the second step of the patient setup. This analysis was made on the kV images acquired at the maximum exhalation phase. The distance shift between the expected and actual fiducial marker positions along the CC direction was estimated for 10 liver patients using the Offline Review application (Varian Medical System).

3. Results

For the 10 patients with liver cancer included in the study, a total of 2705 intrafraction kV images were analyzed for the first 5 fractions of the treatment. For one fraction, the total number of intrafraction kV images acquired during treatment ranged from 8 to 99, mainly depending on the breathing signal changes (Table 2). Table 2 and Fig. 5 present the estimated intrafractional fiducial marker displacement along the CC direction at the maximum exhalation phase compared to their reference positions for all patients.

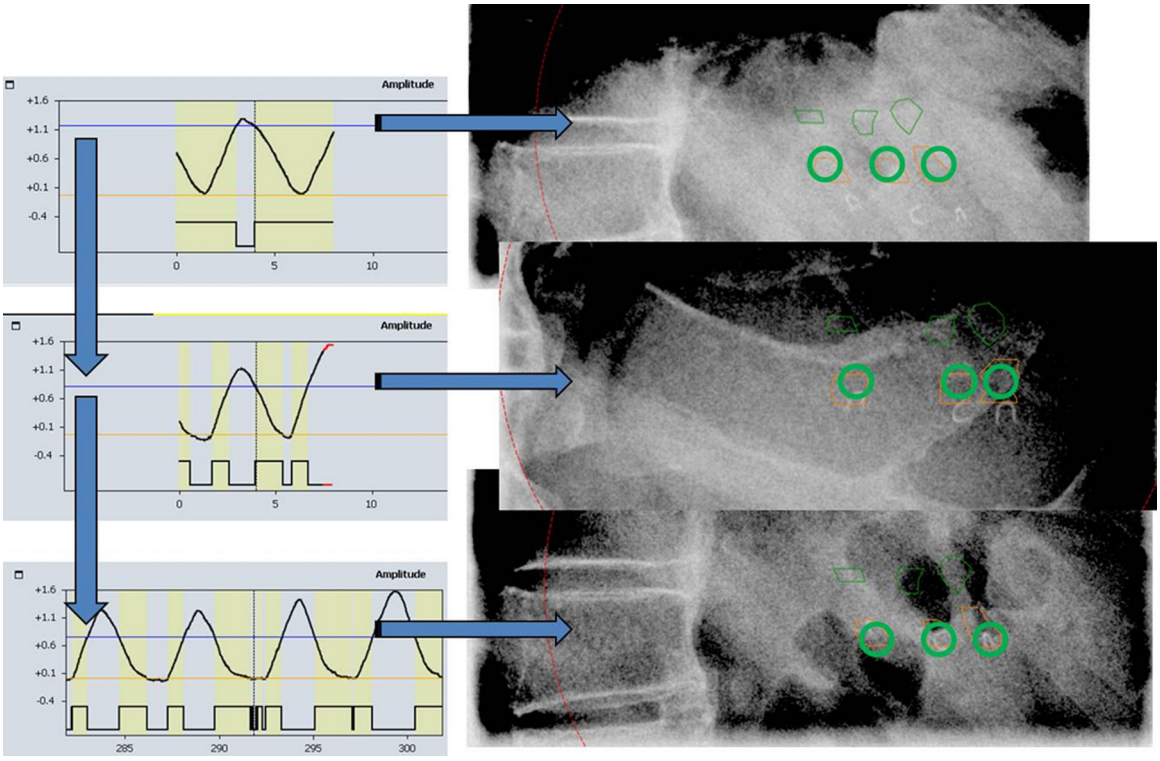

Fig. 3 – Adjustment of the gating threshold performed at the maximum inhalation phase.

The mean ($x_{mean} \pm$ SD mm) intrafractional fiducial marker displacement along the CC direction was -0.1 ± 1.4 mm with a 95% confidence interval of [−2.9, 2.6 mm]. The mean absolute intrafractional fiducial marker deviation at the maximum exhalation phase was 1 mm (Table 3 and Fig. 6a and b).

In 99%, 95% and 90% cases, the deviations of the fiducial markers were ≤4.5 mm, 2.8 mm and 2.2 mm, respectively (Fig. 6b).

4. Discussion

We have presented our gated VMAT liver SBRT protocol using implanted fiducial markers and intrafraction kV images acquired at the beginning of the beam delivery at every breathing cycle during treatment (*i.e.* 2 kV images per breathing cycle at maximum exhalation and inhalation phases). Our study was based on the amplitude-based respiratory gating with

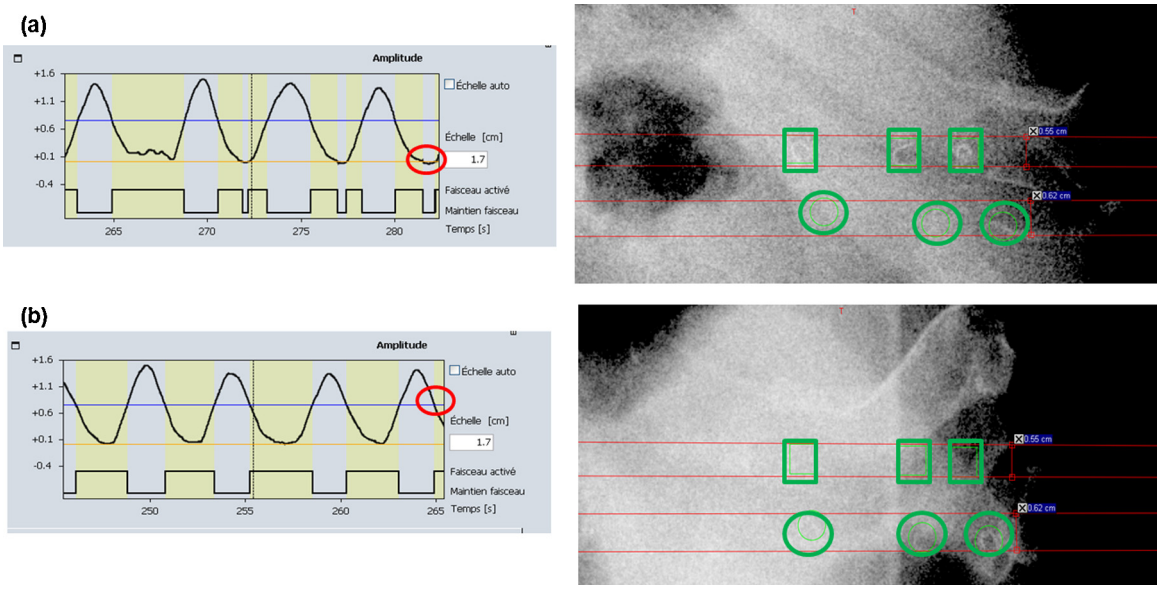

Fig. 4 – kV images acquired at each breathing cycle before MV beam-on at the maximum exhalation (a) and inhalation phase (b).

Table 2 – Total number of kV images acquired and intrafractional fiducial marker displacement along the CC direction for the 10 patients.

Patient index	Total number of kV images for one fraction		Total number of kV images for the five fractions	Intrafractional fiducial marker displacement along the CC direction at the maximum exhalation phase (mm)				
	Min	Max		Min (caudal)	Max (cranio)	Motion range	Mean (x_{mean})	SD (σ)
1	62	84	362	−4.3	1.7	6.0	−0.5	0.9
2	45	99	329	−5.6	5.7	11.3	−0.2	1.9
3	52	92	339	−3.9	5.2	9.1	−0.2	1.7
4	8	72	239	−3.2	7.5	10.7	0.3	1.9
5	26	57	205	−1.9	2.0	3.9	0.2	0.8
6	24	65	245	−3.2	2.0	5.2	−0.7	1.2
7	38	70	285	−3.0	3.0	6.0	−0.2	0.7
8	37	55	235	−3.3	6.3	9.6	0.4	1.3
9	29	86	310	−3.0	2.5	5.5	0.0	1.0
10	18	41	156	−2.5	3.0	5.5	0.0	1.0

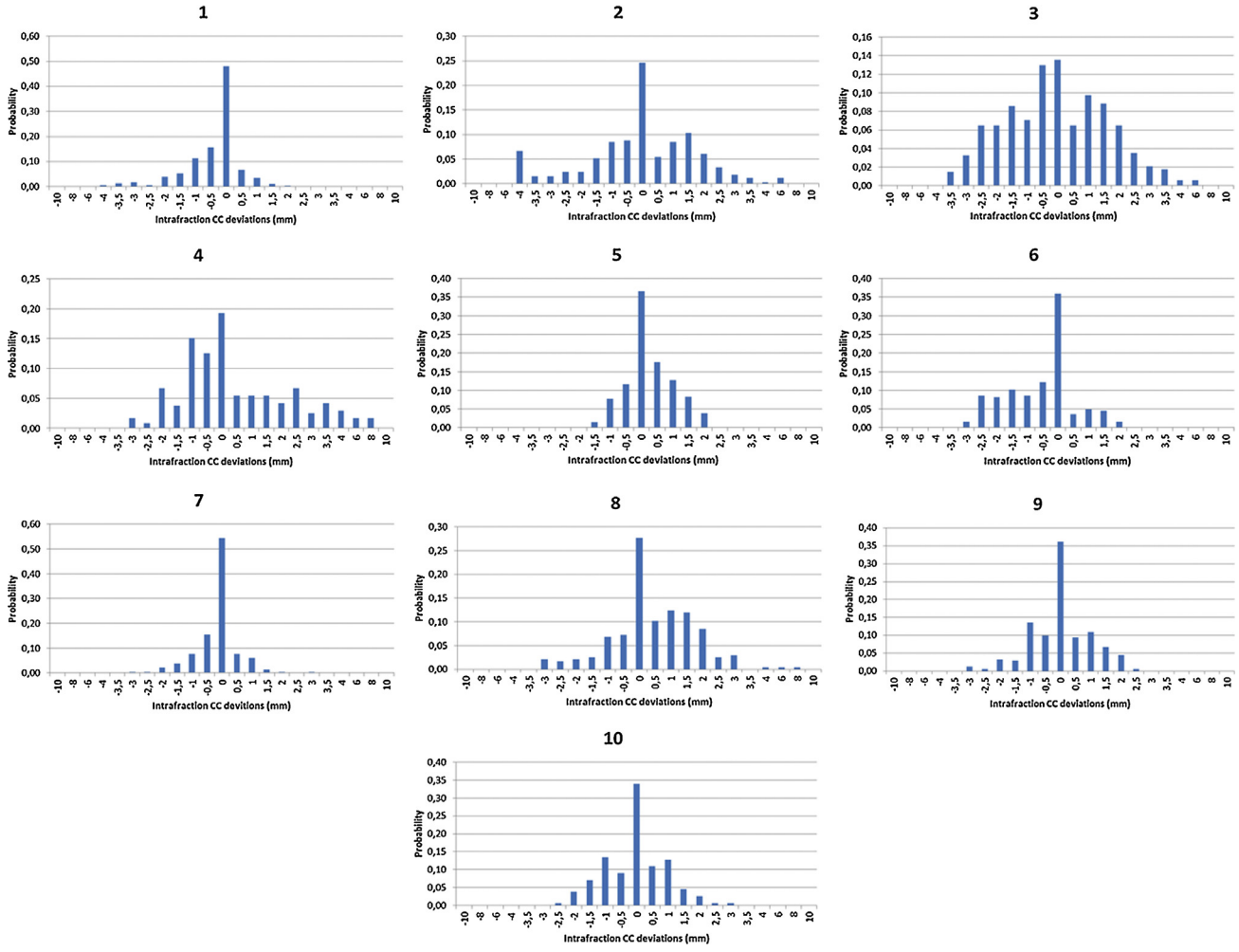

Fig. 5 – Frequency distributions of the fiducial marker displacement along the CC direction ordered by patient number.

daily adjustment of the gating parameters. The present article aimed to describe the evaluation of the fiducial position reproducibility at the maximum exhalation phase.

In liver SBRT, the use of fiducial markers is major to control the respiration-induced motion during the treatment. Many studies on liver motion characterization using markers have been published.[12,16,19] Seppenwoolde et al. showed that the tumor position can be accurately predicted using implanted markers considering that there is a real influence of the marker-tumor distance on the set-up accuracy. They also showed that the diaphragm dome was the second best predictor of tumor motion and that it could be used as a

Table 3 – Intrafractional fiducial marker displacement along the CC direction for the 10 patients' data combined.

Total number of kV images analyzed	Intrafractional fiducial marker displacement along the CC direction at the maximum exhalation phase (mm)					
	Min (caudal)	Max (cranio)	Mean (x_{mean})	Mean absolute deviation	SD (σ)	Confidence interval (95%) [$x_{mean} - 2\sigma$, $x_{mean} + 2\sigma$]
2705	−5.6	7.5	−0.1	1.0	1.4	[−2.9, 2.6]

surrogate for tumor located close to it.[19] Park et al. studied the liver motion characteristics based on fiducial markers tracked with the X-rays projections of the CBCT scans. Their results showed large variations in liver motion and their conclusion was similar to those of Seppenwoolde et al., mainly that the distance between the markers and the tumor was a major element to track.[12] Intrafraction kV images can be used to control and verify the fiducial marker positions during treatment delivery.[17] These images allowed us to ensure the consistency of tumor repositioning during the treatment by frequently controlling the external–internal correlation model. Beddar et al. investigated the correlation between the motions of an external marker and of internal fiducials markers implanted in the liver for 8 patients undergoing 4DCT. They specified that there often was a good correlation between the internal fiducial marker motion imaged by 4DCT and the external marker motion, and that they were best correlated during expiration.[10] Our results thus confirm those of Beddar et al.

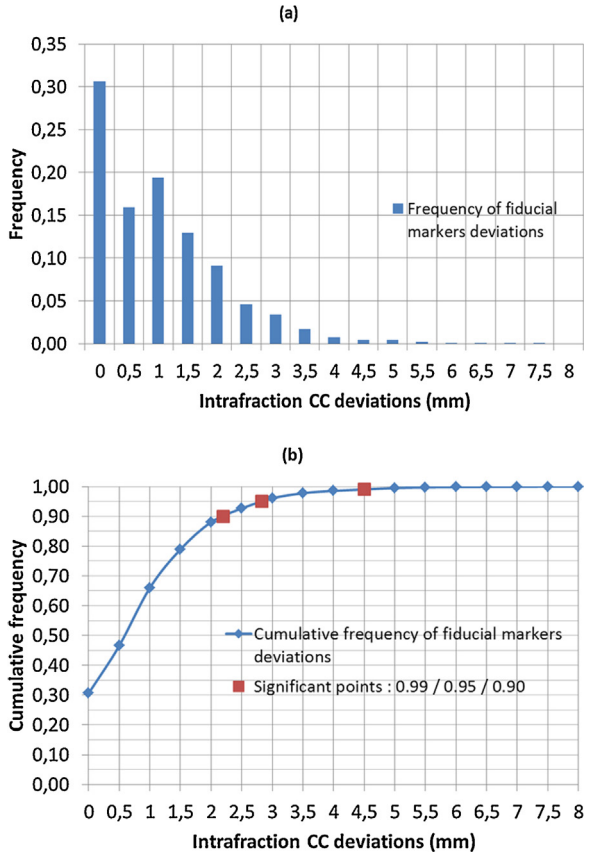

Fig. 6 – (a) Frequency and (b) cumulative frequency of all intrafraction displacement along the CC direction for the 10 patient's data combined.

according to whom actual and expected positions of the fiducial markers at the maximum exhalation phase are generally well concordant (Fig. 5). These frequency distributions showed that there is an accurate patient's alignment reproducibility at the maximum exhalation phase. Indeed, in our protocol, if the fiducial markers shifted during the treatment because of the patient's movements or intrafractional organ motions, the patient was re-aligned. This explains why our frequency distributions were centered to the expected position of the fiducial markers in CC. However, we also observed some deviations. Results showed that in 99% cases, the fiducial marker deviations at the maximum exhalation phase were ≤4.5 mm with a 95% confidence interval of [−2.9, 2.6 mm].[20] These results are in accordance with our ITV/PTV margin protocol, indicating that it seemed to be well adapted to the gated VMAT SBRT treatment in liver disease. Moreover, they are close to the recommendation reported by Ge et al. to use at least a 2.5 mm safety margin to account for gating and setup uncertainties.[8] Li et al. reported results from 5 patients (2 pancreas, 2 livers and 1 lung) using intrafraction kV images verification of gated VMAT. They obtained average intrafraction positioning errors for the 5 patients of 0.8, 0.9 and 1.4 mm in the LR, AP and CC directions, respectively. The errors in the CC direction appeared to be a dominant factor for lung and liver patients.[17]

In a recent study, Winter et al. quantified random uncertainties in robotic radiosurgical treatment of liver lesions with real-time respiratory motion management by analyzing logged tracking information and isolated X-rays images collected before beam delivery. They estimated the overall random uncertainty by quadratically summing correlation determined by periodic X-ray imaging, prediction, and end-to-end targeting errors. They particularly showed that the 95th percentile absolute correlation errors were of 3.3 mm in the cranio-caudal direction, whereas the 95th percentile absolute radial prediction errors were of 0.5 mm. The overall 95th percentile random uncertainty was of 4 mm in the radial direction. They demonstrated that model correlation errors are the primary random source of uncertainty in Cyberknife liver treatment and they suggested that the target should be within 4 mm of the target volume for 95% of the beam delivery.[21] These results coming from another SBRT technique are close to those we obtained with our ITV/PTV margin protocol. In our study, 95% of the deviations of the fiducial markers were ≤2.8 mm.

Our liver treatment protocol was recently improved by including the use of the Automatic Beam-Hold software (ABH, Varian Medical Systems). The ABH algorithm allows the automatic detection of the fiducial markers on the intrafraction kV images, turning on or holding off the MV beam automatically if the markers were in a good or displaced position, respectively. This improvement leads to new questions, such as the

eventuality to treat patients only during the end of the expiratory phases thus minimizing ITV and decreasing the ITV/PTV safety margin to better protect the surrounding healthy tissue.

A shortcoming of this method is that the MV beam is turned off during the majority of the respiratory cycle (*i.e.* loss of duty cycle), resulting in an increase of the treatment time. Nevertheless, a faster delivery of the dose is allowed by the recent development of the Flattening Filter Free beams with a dose rate up to 1400 monitor units/min for 6 MV beams.[22,23] Vassiliev et al. assessed the feasibility of stereotactic radiotherapy for early stage lung cancer using photon beams without a flattening filter. They showed that the total beam-on time was reduced by factor of 2.31 (±0.02 SD) for plans using only 6 MV beams with the filter removed, increasing the feasibility and the efficiency of gated treatments.[24] The next challenge is to treat the patients with liver disease with a gated VMAT SBRT technique including an end-exhalation phase (40–50–60%) gating and Flattening Filter Free beams.

5. Conclusion

This study presented our gated VMAT liver SBRT protocol based on the use of implanted fiducial markers and intrafraction kV images. Tumor repositioning was evaluated thanks to the analysis of intrafraction kV images. We show that in 99% cases, the fiducial marker deviations were ≤4.5 mm in exhalation phase corresponding to our 5 mm ITV/PTV margin. This margin seems to be well adapted to the gated VMAT liver SBRT treatment. The use of intrafraction kV images is crucial to verify the consistency of the correlation between an external surrogate and an internal target motion during the dose delivery.

Conflict of interest

None declared.

Financial disclosure

None declared.

Acknowledgement

Authors thanks Hélène de Forges for her editorial assistance.

REFERENCES

1. Benedict SH, Yenice KM, Followill D, et al. Stereotactic body radiation therapy: the report of AAPM Task Group 101. *Med Phys* 2010;**37**(8):4078, http://dx.doi.org/10.1118/1.3438081.
2. Shirato H, Seppenwoolde Y, Kitamura K, Onimura R, Shimizu S. Intrafractional tumor motion: lung and liver. *Semin Radiat Oncol* 2004;**14**(1):10–8, http://dx.doi.org/10.1053/j.semradonc.2003.10.008.
3. Kitamura K, Shirato H, Seppenwoolde Y, et al. Tumor location, cirrhosis, and surgical history contribute to tumor movement in the liver, as measured during stereotactic irradiation using a real-time tumor-tracking radiotherapy system. *Int J Radiat Oncol* 2003;**56**(1):221–8, http://dx.doi.org/10.1016/S0360-3016(03)00082-8.
4. Eccles C, Brock KK, Bissonnette J-P, Hawkins M, Dawson LA. Reproducibility of liver position using active breathing coordinator for liver cancer radiotherapy. *Int J Radiat Oncol* 2006;**64**(3):751–9, http://dx.doi.org/10.1016/j.ijrobp.2005.05.066.
5. Keall PJ, Mageras GS, Balter JM, et al. The management of respiratory motion in radiation oncology report of AAPM Task Group 76. *Med Phys* 2006;**33**(10):3874, http://dx.doi.org/10.1118/1.2349696.
6. Heinzerling JH, Anderson JF, Papiez L, et al. Four-dimensional computed tomography scan analysis of tumor and organ motion at varying levels of abdominal compression during stereotactic treatment of lung and liver. *Int J Radiat Oncol* 2008;**70**(5):1571–8, http://dx.doi.org/10.1016/j.ijrobp.2007.12.023.
7. Wunderink W, Méndez Romero A, de Kruijf W, de Boer H, Levendag P, Heijmen B. Reduction of respiratory liver tumor motion by abdominal compression in stereotactic body frame, analyzed by tracking fiducial markers implanted in liver. *Int J Radiat Oncol* 2008;**71**(3):907–15, http://dx.doi.org/10.1016/j.ijrobp.2008.03.010.
8. Ge J, Santanam L, Yang D, Parikh PJ. Accuracy and consistency of respiratory gating in abdominal cancer patients. *Int J Radiat Oncol* 2013;**85**(3):854–61, http://dx.doi.org/10.1016/j.ijrobp.2012.05.006.
9. Lu X-Q, Shanmugham LN, Mahadevan A, et al. Organ deformation and dose coverage in robotic respiratory-tracking radiotherapy. *Int J Radiat Oncol* 2008;**71**(1):281–9, http://dx.doi.org/10.1016/j.ijrobp.2007.12.042.
10. Beddar AS, Kainz K, Briere TM, et al. Correlation between internal fiducial tumor motion and external marker motion for liver tumors imaged with 4D-CT. *Int J Radiat Oncol* 2007;**67**(2):630–8, http://dx.doi.org/10.1016/j.ijrobp.2006.10.007.
11. Case RB, Moseley DJ, Sonke JJ, et al. Interfraction and intrafraction changes in amplitude of breathing motion in stereotactic liver radiotherapy. *Int J Radiat Oncol* 2010;**77**(3):918–25, http://dx.doi.org/10.1016/j.ijrobp.2009.09.008.
12. Park JC, Park SH, Kim JH, et al. Liver motion during cone beam computed tomography guided stereotactic body radiation therapy. *Med Phys* 2012;**39**(10):6431, http://dx.doi.org/10.1118/1.4754658.
13. Worm ES, Høyer M, Fledelius W, Poulsen PR. Three-dimensional, time-resolved, intrafraction motion monitoring throughout stereotactic liver radiation therapy on a conventional linear accelerator. *Int J Radiat Oncol* 2013;**86**(1):190–7, http://dx.doi.org/10.1016/j.ijrobp.2012.12.017.
14. Poulsen PR, Worm ES, Petersen JBB, Grau C, Fledelius W, Høyer M. Kilovoltage intrafraction motion monitoring and target dose reconstruction for stereotactic volumetric modulated arc therapy of tumors in the liver. *Radiother Oncol* 2014;**111**(3):424–30, http://dx.doi.org/10.1016/j.radonc.2014.05.007.
15. Kirilova A, Lockwood G, Choi P, et al. Three-dimensional motion of liver tumors using cine-magnetic resonance imaging. *Int J Radiat Oncol* 2008;**71**(4):1189–95, http://dx.doi.org/10.1016/j.ijrobp.2007.11.026.
16. Wunderink W, Méndez Romero A, Seppenwoolde Y, de Boer H, Levendag P, Heijmen B. Potentials and limitations of guiding liver stereotactic body radiation therapy set-up on liver-implanted fiducial markers. *Int J Radiat Oncol* 2010;**77**(5):1573–83, http://dx.doi.org/10.1016/j.ijrobp.2009.10.040.

17. Li R, Mok E, Han B, Koong A, Xing L. Evaluation of the geometric accuracy of surrogate-based gated VMAT using intrafraction kilovoltage X-ray images. *Med Phys* 2012;**39**(5):2686, http://dx.doi.org/10.1118/1.4704729.
18. Crocker JK, Ng JA, Keall PJ, Booth JT. Measurement of patient imaging dose for real-time kilovoltage X-ray intrafraction tumour position monitoring in prostate patients. *Phys Med Biol* 2012;**57**(10):2969–80, http://dx.doi.org/10.1088/0031-9155/57/10/2969.
19. Seppenwoolde Y, Wunderink W, Veen SRW, Storchi P, Romero AM, Heijmen BJM. Treatment precision of image-guided liver SBRT using implanted fiducial markers depends on marker–tumour distance. *Phys Med Biol* 2011;**56**(17):5445–68, http://dx.doi.org/10.1088/0031-9155/56/17/001.
20. Vanherk M. Errors and margins in radiotherapy. *Semin Radiat Oncol* 2004;**14**(1):52–64, http://dx.doi.org/10.1053/j.semradonc.2003.10.003.
21. Winter JD, Wong R, Swaminath A, Chow T. Accuracy of robotic radiosurgical liver treatment throughout the respiratory cycle. *Int J Radiat Oncol* 2015;**93**(4):916–24, http://dx.doi.org/10.1016/j.ijrobp.2015.08.031.
22. Vassiliev ON, Titt U, Pönisch F, Kry SF, Mohan R, Gillin MT. Dosimetric properties of photon beams from a flattening filter free clinical accelerator. *Phys Med Biol* 2006;**51**(7):1907–17, http://dx.doi.org/10.1088/0031-9155/51/7/019.
23. Hrbacek J, Lang S, Klöck S. Commissioning of photon beams of a flattening filter-free linear accelerator and the accuracy of beam modeling using an anisotropic analytical algorithm. *Int J Radiat Oncol* 2011;**80**(4):1228–37, http://dx.doi.org/10.1016/j.ijrobp.2010.09.050.
24. Vassiliev ON, Kry SF, Chang JY, Balter PA, Titt U, Mohan R. Stereotactic radiotherapy for lung cancer using a flattening filter free Clinac. *J Appl Clin Med Phys* 2009;**10**(1).